·基础研究·

从海马区胶质细胞CD137L途径探讨电针治疗神经痛的作用机制

郑昌岳[1],兰艳艳[2],黄秋玲[2],江孟鸿[3],王志福[2*]

1 福建省级机关医院,福建 福州 350003;
2 福建中医药大学附属康复医院,福建 福州 350003;
3 福建中医药大学针灸学院,福建 福州 350122
* 通信作者:王志福,E-mail:2007015@fjtcm.edu.cn

收稿日期:2023-02-19;接受日期:2023-05-27
基金项目:国家自然科学基金面上项目(82274658)
DOI:10.3724/SP.J.1329.2023.05005
开放科学(资源服务)标识码(OSID):

摘要 **目的:**探讨海马CA1区胶质细胞CD137L在电针改善神经痛大鼠机械痛及学习记忆障碍的作用机制。**方法:**将24只SD大鼠按照随机数字表法分为假手术组、模型组和电针组,每组8只。模型组和电针组制备坐骨神经分支选择性损伤(SNI)神经痛模型;假手术组只暴露坐骨神经,但不结扎。造模后第7天开始,电针组对右侧环跳、阳陵泉穴予以电针刺激,频率2 Hz,强度1 mA,每天1次,每次30 min,连续21 d;假手术组和模型组同等条件抓取、固定,但不进行任何干预。SD大鼠造模前及造模后第28天,用Von-Frey测痛仪检测机械痛阈值;造模后28 d采用新物体识别实验检测大鼠学习记忆能力;酶联免疫吸附法检测海马CA1区CD137L、胶质细胞活化标记物(Iba-1、GFAP)和肿瘤坏死因子-α(TNF-α)的浓度;免疫荧光组织化学法检测海马CA1区CD137L及其受体CD137在神经细胞的表达定位情况。**结果:**① 与假手术组比较,模型组机械痛阈值和新物体识别指数均显著降低($P<0.01$);与模型组比较,电针组机械痛阈值和新物体识别指数均显著升高($P<0.01$)。② 与假手术组比较,模型组海马CD137L、Iba-1、GFAP和TNF-α浓度均显著升高($P<0.01$),Iba-1和GFAP免疫反应阳性个数明显增多(P均<0.01);与模型组比较,电针组海马CD137L、Iba-1、GFAP和TNF-α浓度均显著下降(P均<0.05),Iba-1和GFAP免疫反应阳性个数均明显减少($P<0.01$)。③ 免疫荧光检测发现,海马CA1区CD137L及其受体CD137与Iba-1、GFAP共表达明显,提示CD137L及其受体CD137主要表达于小胶质细胞、星形胶质细胞,但不表达于神经元。**结论:**电针可能下调海马CA1区胶质细胞CD137L表达,抑制胶质细胞的活化和TNF-α的释放,减轻神经痛大鼠疼痛及学习记忆障碍。

关键词 神经痛;海马;CD137L;胶质细胞;电针

神经病理性疼痛(简称神经痛)是躯体感觉系统的损害或疾病导致的疼痛,临床表现为痛觉过敏、痛觉超敏等症状,并常伴随记忆障碍[1-3]。海马作为大脑内侧颞叶的一部分,在伤害性刺激的感受以及疼痛信号的处理过程中发挥重要作用[4]。神经痛发生时,海马功能呈现出不同寻常的表现,如记忆缺陷、胶质细胞激活和细胞因子释放等[5-7]。CA1区作为海马重要的功能分区之一,在痛觉调制和突触可塑性过程中同样扮演着重要角色[8],疼痛信息可诱导CA1区蛋白表达和细胞功能的改变,如肿瘤坏死因子-α(tumor necrosis factor-α,TNF-α)释放等[9-11]。

引用格式:郑昌岳,兰艳艳,黄秋玲,等. 从海马区胶质细胞CD137L途径探讨电针治疗神经痛的作用机制[J]. 康复学报,2023,33(5):419-427.
ZHENG C Y,LAN Y Y,HUANG Q L,et al. Mechanism of electroacupuncture on neuropathic pain via regulation of CD137L in hippocampus glia [J]. Rehabil Med,2023,33(5):419-427.
DOI:10.3724/SP.J.1329.2023.05005

大量研究证实，电针环跳、阳陵泉穴可显著抑制神经痛，在海马CA1区观察发现，电针可以减少神经痛大鼠疼痛相关神经元电生理活动的异常[12]。前期研究通过蛋白组学筛查发现，电针可抑制海马关键蛋白TMEM126A的表达，减轻神经痛敏反应，改善相关学习记忆障碍，而CD137L是TMEM126A的重要结合蛋白[13-15]。通过文献进一步梳理分析，CD137属于肿瘤坏死因子(tumor necrosis factor，TNF)受体家族的成员，由肿瘤坏死因子受体超家族成员9(tumor necrosis factor receptor superfamily member 9，TNFRSF9)基因编码。CD137是在活化的$CD4^+$和$CD8^+$ T细胞、NK细胞、DC、巨噬细胞、肥大细胞等细胞上表达的诱导型共刺激受体，其配体为CD137L，表达于巨噬细胞、B细胞等。

在神经痛研究中发现，敲除CD137L基因的小鼠疼痛阈值升高，并且早期使用CD137L抗体能够有效改善痛敏反应；脊髓节段CD137L可能通过调节小胶质细胞的活化和细胞因子的释放，促进神经痛的发生和发展[16]。然而，目前关于CD137及配体CD137L中枢神经表达及电针镇痛的作用机制不清。基于此，拟探讨海马CD137及CD137L在电针改善神经痛及学习记忆中的作用。

1 实验材料

1.1 实验动物

24只SPF级雄性SD大鼠，体质量160～180 g，购自浙江省医学科学院[许可证号：SCXK(浙)2019-0002]，饲养于福建中医药大学实验动物中心[许可证号：SYXK(闽)2019-0007]。饲养环境保持适宜的温度、湿度、12 h光照明暗交替。本实验操作过程严格按照我国相关实验动物的规定及福建中医药大学动物管理制度，符合实验动物伦理要求(审批号：FJTCMIACUC2021006)。

1.2 仪器设备和试剂

1.2.1 主要仪器设备 Von-Frey测痛仪(美国IITC公司，型号：NC12775)；电子针疗仪(型号：SDZ-Ⅱ)、一次性针灸针(规格：1寸，0.30 mm×25 mm)均购自于苏州医疗用品厂有限公司；LEICA冰冻切片机(德国徕卡公司，型号：CM1950)；LEICA显微镜(德国徕卡公司，型号：DFC425 C)。

1.2.2 主要试剂 5-0非吸收性外科缝线(上海浦东金环医疗用品股份有限公司)；CD137/CD137L抗体、小胶质细胞标记物(Ionized calcium-binding adapter molecule 1，Iba-1)抗体、星形胶质细胞标记物(Glial Fibrillary Acidic Protein，GFAP)抗体(美国Thermo试剂公司)；GFAP、Iba-1、CD137L、TNF-α等ELISA试剂盒(武汉伊莱瑞特生物科技股份有限公司)。

2 实验方法

2.1 实验分组

24只SPF级雄性SD大鼠适应性喂养1周后，按照随机数字表法分为假手术组、模型组和电针组，每组8只。

2.2 动物模型制备

参考DECOSTERD的造模方法建立坐骨神经分支选择性损伤(spared nerve injury，SNI)模型[17]。大鼠经异氟烷麻醉后，剃除皮毛，75%乙醇消毒，切开右后肢皮肤，钝性分离肌肉，充分暴露坐骨神经主干及其远端分支，钝性分离胫神经、腓总神经和腓肠神经，5-0丝线结扎腓总神经和胫神经并剪断，保留腓肠神经，造模后逐层缝合，切口处覆盖青霉素粉末预防感染。假手术组只暴露坐骨神经，不结扎不剪断坐骨神经及分支。

2.3 干预方法

造模后第7天开始，电针组参照《实验针灸学》及前期研究方法[18]确定大鼠右侧环跳、阳陵泉穴位置，采用常规一次性针灸针(1寸，0.30 mm×25 mm)分别刺入10 mm、5 mm，连接电子针疗仪，电针频率为2 Hz，强度为1 mA，连续波，每天干预1次，每次30 min，连续电针21 d。假手术组和模型组大鼠同等条件下进行抓取、固定，但不给予电针干预。

2.4 行为学检测

2.4.1 机械痛阈值检测 参考前期研究方法[18]进行机械痛阈值测试以及数值计算。在造模前及造模后第7天(干预前)、造模后第28天(干预后)检测3组机械痛阈值。每次刺激后待大鼠重新安静后再开始下一次刺激，测量3次得出的平均值记录为测试结果，代入up-and-down方法的公式计算，最终所得数值即为大鼠缩足阈值(paw withdrawal threshold，PWT)，以此反映大鼠的机械痛行为学。

2.4.2 新物体识别实验 根据啮齿类动物具备对新的物体有探索的偏好本能，在造模后第28天进行新物体识别实验，以反映大鼠的学习记忆能力。① 适应阶段：将动物依次放入测试箱内适应环境。每只大鼠放置在测试箱内10 min任其自由探索，然

后取出放回原笼内休息10 min,再放入测试箱10 min,最后归回原笼位。注意每次更换动物测试前必须清除测试箱内残留的粪便和尿液等,并用75%乙醇喷洒、擦拭、通风以消除气味。② 训练阶段:准备2个完全相同的圆柱体(物体A和物体B),1个长方体(物体C)。3个物体和大鼠的体积匹配并具备一定体质量,以避免在实验过程中因大鼠攀爬而倾倒。先将物体A和物体B放置在测试箱的左下角和右下角,调试视频分析系统并定义物体和环境的区域范围,打开录像设备。将大鼠背对2个物体放入测试箱中。实验人员离开测试房间以避免干扰。大鼠在测试箱内自由探索10 min后,取出放回原笼内,间隔10 min后进行下一阶段。③ 测试阶段:将左下角的物体A取出,换为物体C。打开录像设备,同样放置大鼠进入测试箱。实验人员离开房间,通过录像观察大鼠探索情况,物体识别测试时间为10 min。测试完成后将大鼠归回原笼内。通过视频分析系统采集录像,分析记录大鼠相关指标。

2.5 样本采集

造模后第28天进行样本采集。用1%浓度异氟烷麻醉大鼠后,新鲜快速取脑,分离海马CA1区,置入EP管液氮冻存待取。灌注取材快速灌入低温生理盐水,缓慢灌入低温4%多聚甲醛,取大脑制作冰冻切片。

2.6 酶联免疫吸附法

① 标准品稀释:根据说明书,对标准品进行梯度稀释,混匀备用。② 加样:分别设空白孔、标准品孔、待测样本孔。在酶标包被板上标准品准确加样50 μL,待测样本孔中先加样品稀释液25 μL,再加待测样本25 μL,轻轻晃动混匀。③ 温育:用封板膜封板后置37 ℃温育30 min。④ 配液:将30倍浓缩洗涤液用蒸馏水30倍稀释后备用。⑤ 洗涤:小心揭去封板膜,弃去液体,甩干,每孔加满洗涤液,静置30 s后弃去,如此反复5次,拍干。⑥ 加酶:加入酶标试剂50 μL。⑦ 温育、洗涤:操作同前。⑧ 显色:每孔加入显色剂A 50 μL,再加入显色剂B 50 μL,轻轻震荡混匀,37 ℃避光显色10 min。用450 nm波长分别测量每个孔的吸光值(*A*值)。整个测定的过程应在加入终止液后的15 min内完成。通过Excel绘制标准曲线可以计算出样品浓度值,并进行统计学分析。

2.7 免疫荧光组织化学

实验结束后取材腰段脊髓包埋,在恒冷冻切片机内进行切片,厚度为16 μm,将切好的组织片贴附在载玻片上;将切片PBS洗5 min×3次,用基因笔画圈,滴加封闭液,置于37 ℃恒温箱1 h;甩掉封闭液,分别滴加一抗(小鼠抗Iba-1、小鼠抗GFAP、小鼠抗神经元标记物(Neuronal Nuclei,NeuN)、兔抗CD137、兔抗CD137L),湿盒4 ℃过夜;次日,PBS洗5 min×3次,再避光加入二抗,置于37 ℃箱1 h;PBS洗10 min×3次,擦去组织周围的水分后,滴加含DAPI的封片剂,盖上载玻片。使用荧光显微镜拍摄每只大鼠海马CA1区,每只至少随机选取5个视野拍片,并统计分析。

2.8 统计学方法

所有数据经SPSS 25.0统计分析。计量资料符合正态分布以($\bar{x}\pm s$)表示,多组间比较采用方差分析。不符合正态分布以中位数和四分位数间距[M(P_{25},P_{75})]表示,多组间比较采用非参数秩和检验。以$P<0.05$表示差异具有统计学意义。

3 结 果

3.1 3组机械痛阈值、新物体识别能力比较

3组机械痛阈值采用重复测量方差分析进行统计,数据满足球形检验($P<0.001$),3组主体内时间效应差异具有统计学意义($F=32.54$,$P<0.001$),3组主体间的组别效应差异具有统计学意义($F=31.92$,$P<0.001$),随后进行两两比较。造模后第7天,与假手术组比较,模型组和电针组机械痛阈值均显著下降($P<0.01$)。电针干预21 d后,与模型组相比,电针组可显著提高大鼠机械痛阈值($P<0.01$)。见表1。3组新物体识别指数采用单因素方差分析进行统计,造模后第28天,与假手术组比较,模型组新物体识别指数显著降低($P<0.01$),提示大鼠学习记忆能力显著下降;与模型组比较,电针组新物体识别指数显著升高($P<0.01$),提示大鼠学习记忆能力显著改善。见图1。

表1 3组大鼠机械痛阈值变化($\bar{x}\pm s$)

Table 1 Changes of mechanical pain threshold of rats in three groups ($\bar{x}\pm s$)

组别	n	造模前	造模后第7天	造模后第28天
假手术组	8	10.13±1.77	9.50±1.87	8.78±2.45
模型组	8	9.51±1.32	3.34±1.40[1)]	2.10±0.43[1)]
电针组	8	9.32±1.48	3.77±1.19[1)]	9.80±2.63[2)]

注:与假手术组比较,1) $P<0.01$;与模型组比较,2) $P<0.01$。

Note: Compared with the sham group, 1) $P<0.01$; compared with the model group, 2) $P<0.01$.

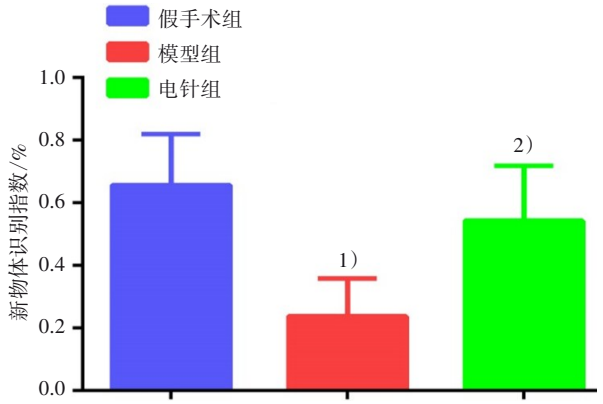

注：与假手术组比较，1）$P<0.01$；与模型组比较，2）$P<0.01$。

Note: Compared with the sham group, 1) $P<0.01$; compared with the model group, 2) $P<0.01$.

图 1　3 组大鼠新物体识别指数比较（$\bar{x}\pm s$）

Figure 1　Comparison of new object recognition in dex in three groups ($\bar{x}\pm s$)

3.2　3 组大鼠海马 CA1 区 CD137、CD137L 与神经细胞共表达情况

免疫荧光检测表明，海马 CA1 区 CD137 免疫反应阳性物质与 Iba-1、GFAP 免疫反应阳性物质共标记，而与 NeuN 免疫反应阳性物质未共标记。见图 2。同样，在海马 CA1 区，CD137L 免疫反应阳性物质与 Iba-1、GFAP 共标记，而与 NeuN 未共标记。见图 3。

3.3　3 组海马 CA1 区 CD137L 浓度的比较

造模后第 28 天，采用 ELISA 检测大鼠海马 CA1 区 CD137L 浓度。与假手术组比较，模型组 CD137L 浓度显著上升（$P<0.01$）；与模型组比较，电针组 CD137L 浓度显著下降（$P<0.01$），见图 4。

3.4　3 组海马 CA1 区 Iba-1、GFAP 蛋白表达的比较

造模后第 28 天，采用免疫荧光和 ELISA 测定 3 组海马 CA1 区小胶质细胞和星形胶质细胞激活标记物的表达。与假手术组比较，模型组 Iba-1 免疫反应阳性细胞个数和浓度均明显增多（$P<0.01$）；与模型组比较，电针组 Iba-1 细胞个数和浓度均明显减少（$P<0.01$）。见图 5 和图 6。与假手术组比较，模型组 GFAP 免疫反应阳性细胞个数和浓度均明显增多（$P<0.01$）；与模型组比较，电针组 GFAP 细胞个数和浓度均明显减少（$P<0.01$）。见图 7 和图 8。

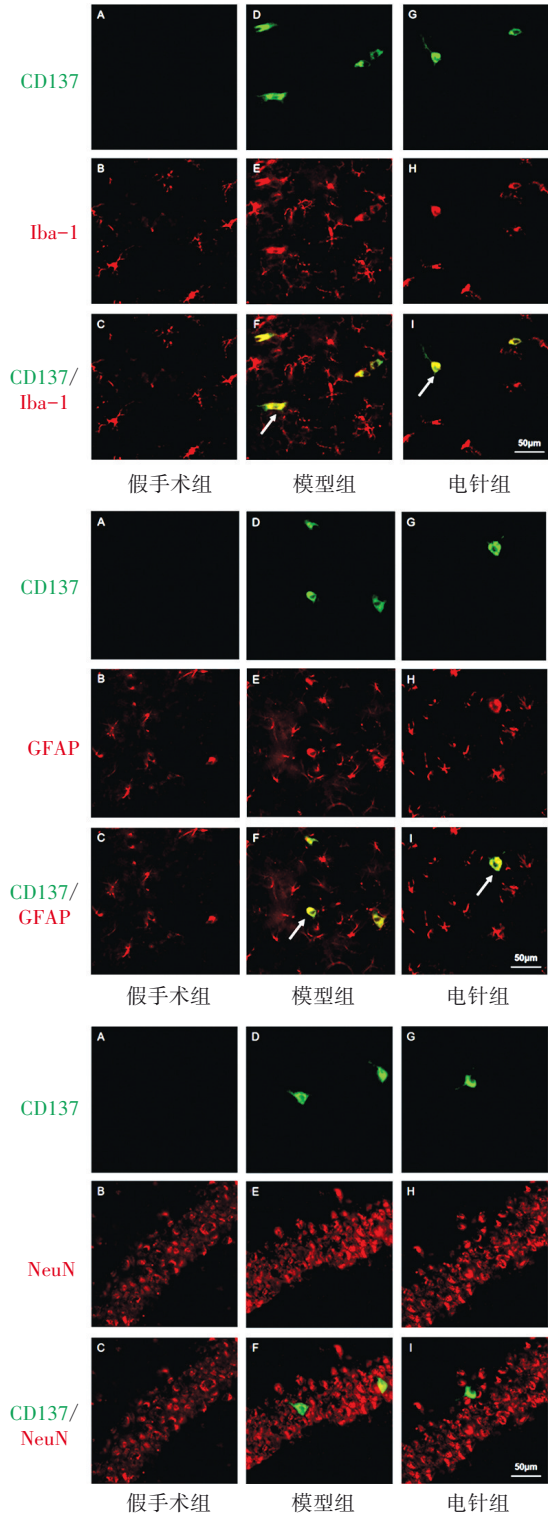

图 2　3 组海马 CA1 区 CD137 和 Iba-1、GFAP、NeuN 免疫荧光共标情况（×400）

Figure 2　Co-labeling of CD137 with Iba-1, GFAP and NeuN immunofluorescence in hippocampal CA1 region of three groups (×400)

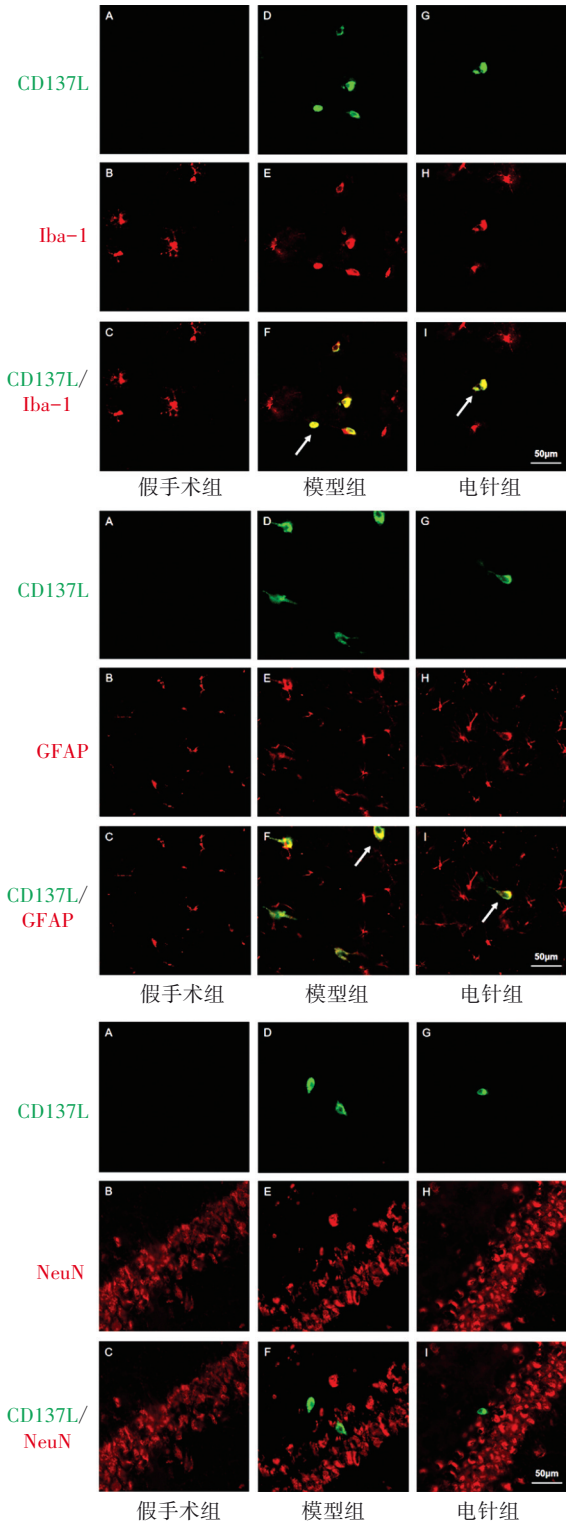

图3　3组海马CA1区CD137L和Iba-1、GFAP、NeuN免疫荧光共标情况(×400)

Figure 3　Co-labeling of CD137L with Iba-1,GFAP and NeuN immunofluorescence in hippocampal CA1 region of three groups (×400)

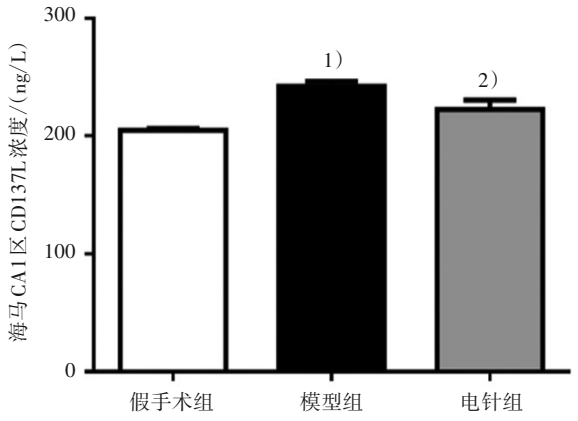

注:与假手术组比较,1) $P<0.01$;与模型组比较,2) $P<0.01$。

Note: Compared with the sham group, 1) $P<0.01$; compared with the model group, 2) $P<0.01$.

图4　3组大鼠海马CA1区CD137L浓度比较

Figure 4　Comparison of CD137L concentration in hippocampal CA1 region in three groups

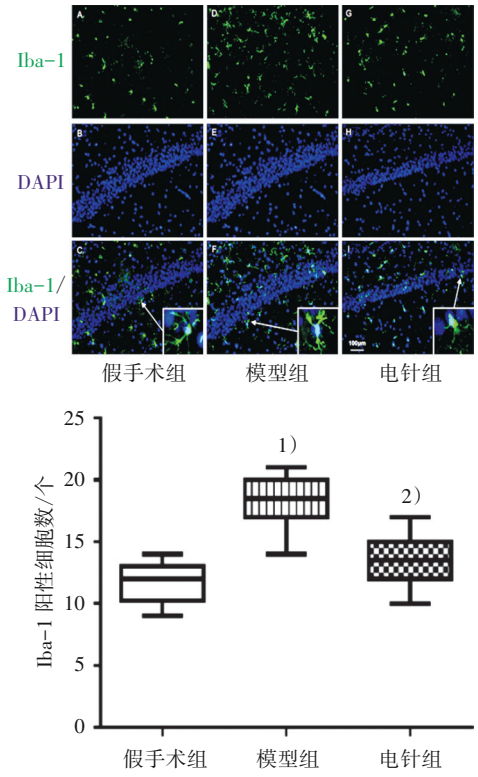

注:与假手术组比较,1) $P<0.01$;与模型组比较,2) $P<0.01$。

Note: Compared with the sham group, 1) $P<0.01$; compared with the model group, 2) $P<0.01$.

图5　3组大鼠海马CA1区小胶质细胞标记物Iba-1表达情况(×200)

Figure 5　Expression of microglia marker Iba-1 in hippocampal CA1 and the number of immunoreactive cells in three groups (×200)

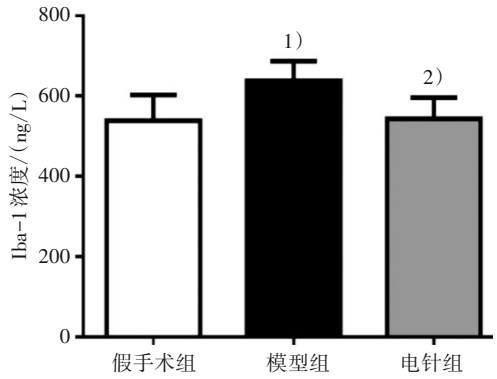

注：与假手术组比较，1）$P<0.01$；与模型组比较，2）$P<0.01$。

Note: Compared with the sham group, 1) $P<0.01$; compared with the model group, 2) $P<0.01$.

图 6　3 组大鼠海马 CA1 区 Iba-1 含量变化比较

Figure 6　Comparison of Iba-1 content in hippocampal CA1 region of three groups

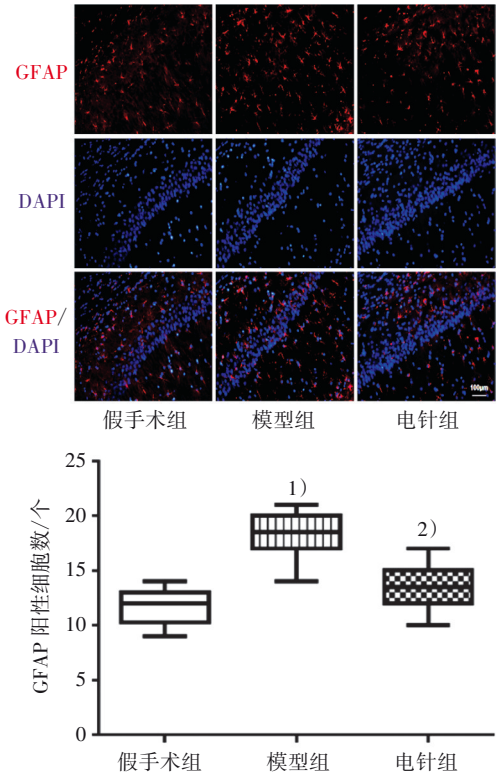

注：与假手术组比较，1）$P<0.01$；与模型组比较，2）$P<0.01$。

Note: Compared with the sham group, 1) $P<0.01$; compared with the model group, 2) $P<0.01$.

图 7　3 组大鼠海马 CA1 区星形胶质细胞标记物 GFAP 表达情况（×200）

Figure 7　Expression of astrocyte marker GFAP in hippocampal CA1 region of three groups (×200)

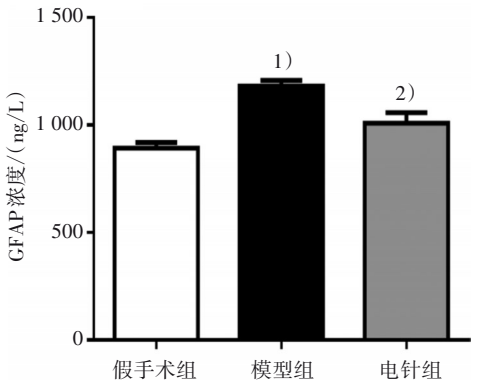

注：与假手术组比较，1）$P<0.01$；与模型组比较，2）$P<0.01$。

Note: Compared with the sham group, 1) $P<0.01$; compared with the model group, 2) $P<0.01$.

图 8　3 组大鼠海马 CA1 区 GFAP 含量变化比较

Figure 8　Comparison of GFAP content of hippocampal CA1 region in three groups

3.5　3 组大鼠海马 CA1 区 TNF-α 释放浓度比较

造模后第 28 天，采用 ELISA 检测大鼠海马 CA1 区 TNF-α 浓度。与假手术组比较，模型组 TNF-α 浓度显著上升（$P<0.01$）；与模型组比较，电针组 TNF-α 浓度显著下降（$P<0.05$）。见图 9。

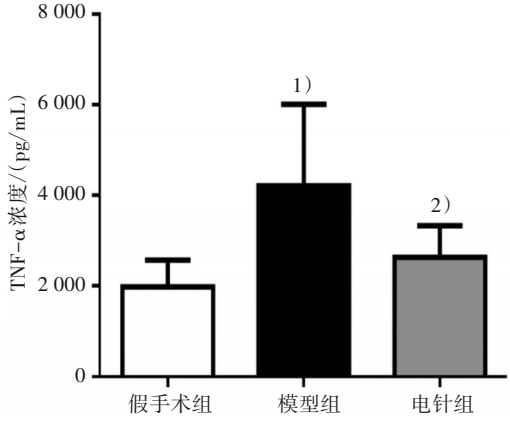

注：与假手术组比较，1）$P<0.01$；与模型组比较，2）$P<0.05$。

Note: Compared with the sham group, 1) $P<0.01$; compared with the model group, 2) $P<0.05$.

图 9　3 组大鼠海马 CA1 区 TNF-α 浓度比较

Figure 9　Comparison of TNF-α concentration in hippocampal CA1 region of three groups

4　讨　论

近年研究表明，海马作为疼痛矩阵脑区的组成之一，是疼痛等伤害性信息加工及修饰的关键脑区，在整合疼痛信息、认知记忆等方面发挥着重要

的作用[19]。神经痛发生时，海马区长时程增强（long-term potentiation，LTP）减弱，小胶质细胞活化及TNF-α释放增多，导致疼痛发生和记忆障碍；抑制海马区胶质细胞活化，降低TNF-α释放，可缓解神经痛[20-22]。

坐骨神经痛归属中医“痛痹证”范畴，应用足少阳经穴环跳、阳陵泉等进行电针，善治诸痛痹不仁，临床康复效果显著。我们前期实验研究同样表明，电针环跳、阳陵泉可显著抑制坐骨神经痛，但关于海马中枢的调控机制仍有待深入明晰[23-25]。

课题组前期蛋白组学筛选发现，电针可显著提高神经痛海马区TMEM126A表达。进一步文献梳理发现，TMEM126A可能结合CD137L结合，在神经痛及电针干预中扮演重要角色[14]。基于此，本研究将CD137L及其受体CD137作为电针干预神经痛的可能作用靶点[26]。实验研究表明，海马CA1区CD137L及其受体主要表达于胶质细胞，电针可显著抑制神经痛海马区CD137L表达和胶质细胞活化，降低炎症因子TNF-α的释放。

CD137又称4-1BB，是一种有效的T细胞共刺激分子，在活化T细胞、NK细胞和血管内皮细胞上表达。其配体CD137L是一种跨膜蛋白，在活化的抗原提呈细胞（antigen presenting cell，APC）上与CD137结合，并将激活信号传递到APC中[27]。CD137-CD137L的主要功能是调节细胞存活，抑制二者结合可阻止肿瘤坏死因子受体（tumor necrosis factor receptors，TNFRs）下游信号通路的激活，降低免疫炎症反应[28-29]。

然而，CD137和CD137L在疼痛疾病中的探索尚属于起步阶段。WAKLEY等[16]研究发现，基因敲除CD137L的神经痛小鼠表现出显著的痛敏反应，早期鞘内注射CD137L抗体提高机械痛阈值，抑制脊髓小胶质细胞炎症反应。体内外实验发现，小胶质细胞与CD137L共表达，激活小胶质细胞，诱导炎症因子如TNF-α等的释放[30]。在炎症状态下，CD137L是巨噬细胞持续产生TNF-α所必需的关键蛋白；巨噬细胞表达CD137L，与Toll样受体相互作用，维持TNF-α产生[31]。

综上所述，电针可能是通过海马CA1区CD137L调节途径，抑制胶质细胞的激活和TNF-α的释放，改善神经痛大鼠疼痛及其学习记忆障碍，今后将通过CD137L及受体病毒干扰、基因敲除等技术，进一步深入验证CD137L/CD137在电针抗炎镇痛中的中枢作用机制。

参考文献

[1] FINNERUP N B, KUNER R, JENSEN T S. Neuropathic pain: from mechanisms to treatment [J]. Physiol Rev, 2021, 101(1): 259-301.

[2] COLLOCA L, LUDMAN T, BOUHASSIRA D, et al. Neuropathic pain [J]. Nat Rev Dis Primers, 2017, 3: 17002.

[3] XIA S H, HU S W, GE D G, et al. Chronic pain impairs memory formation via disruption of neurogenesis mediated by mesohippocampal brain-derived neurotrophic factor signaling [J]. Biol Psychiatry, 2020, 88(8): 597-610.

[4] VASIC V, SCHMIDT M H H. Resilience and vulnerability to pain and inflammation in the hippocampus [J]. Int J Mol Sci, 2017, 18(4): 739.

[5] REN W J, LIU Y, ZHOU L J, et al. Peripheral nerve injury leads to working memory deficits and dysfunction of the hippocampus by upregulation of TNF-α in rodents [J]. Neuropsychopharmacology, 2011, 36(5): 979-992.

[6] HISAOKA-NAKASHIMA K, OHATA K, YOSHIMOTO N, et al. High-mobility group box 1-mediated hippocampal microglial activation induces cognitive impairment in mice with neuropathic pain [J]. Exp Neurol, 2022, 355: 114146.

[7] REY A D, YAU H J, RANDOLF A, et al. Chronic neuropathic pain-like behavior correlates with IL-1β expression and disrupts cytokine interactions in the hippocampus [J]. Pain, 2011, 152(12): 2827-2835.

[8] ALKADHI K A. Cellular and molecular differences between area CA1 and the dentate gyrus of the hippocampus [J]. Mol Neurobiol, 2019, 56(9): 6566-6580.

[9] SAFFARPOUR S, SHAABANI M, NAGHDI N, et al. *In vivo* evaluation of the hippocampal glutamate, GABA and the BDNF levels associated with spatial memory performance in a rodent model of neuropathic pain [J]. Physiol Behav, 2017, 175: 97-103.

[10] GONG W Y, WANG R, LIU Y, et al. Chronic monoarthritis pain accelerates the processes of cognitive impairment and increases the NMDAR subunits NR2B in CA3 of hippocampus from 5-month-old transgenic APP/PS1 mice [J]. Front Aging Neurosci, 2017, 9: 123.

[11] MA L Y, YUE L P, ZHANG Y Q, et al. Spontaneous pain disrupts ventral hippocampal CA1-infralimbic cortex connectivity and modulates pain progression in rats with peripheral inflammation [J]. Cell Rep, 2019, 29(6): 1579-1593. e6.

[12] WANG J Y, CHEN R B, CHEN S P, et al. Electroacupuncture reduces the effects of acute noxious stimulation on the electrical activity of pain-related neurons in the hippocampus of control and neuropathic pain rats [J]. Neural Plast, 2016, 2016: 6521026.

[13] SUN H F, YANG X L, ZHAO Y, et al. Loss of TMEM126A promotes extracellular matrix remodeling, epithelial-to-mesenchymal transition, and breast cancer metastasis by regulating mitochondrial retrograde signaling [J]. Cancer Lett, 2019, 440/441: 189-201.

[14] KIM E C, MOON J H, KANG S W, et al. TMEM126A, a CD137 ligand binding protein, couples with the TLR4 signal transduction pathway in macrophages [J]. Mol Immunol, 2015, 64(2): 244-251.

[15] BAE, CHOI J K, MOON J H, et al. Novel transmembrane protein 126A (TMEM126A) couples with CD137L reverse signals in myeloid cells [J]. Cell Signal, 2012, 24(12): 2227-2236.

[16] WAKLEY A A, LEEMING R, MALON J, et al. Contribution of CD137L to sensory hypersensitivity in a murine model of neuropathic pain [J]. eNeuro, 2018, 5(5): ENEURO. 0218-ENEURO. 0218. 2018.

[17] LIU S, MI W L, LI Q, et al. Spinal IL-33/ST2 signaling contributes to neuropathic pain via neuronal CaMK Ⅱ-CREB and astroglial JAK2-STAT3 cascades in mice [J]. Anesthesiology, 2015, 123(5): 1154-1169.

[18] 王志福,俞向梅,龚德贵,等. 电针"阳陵泉""环跳"对神经病理性疼痛大鼠脊髓SOCS3的影响[J]. 中国疼痛医学杂志, 2015, 21(5): 335-340.
WANG Z F, YU X M, GONG D G, et al. Effects of electroacupuncture at "Yanglinquan" and "Huantiao" acupoints on expression of SOCS3 in spinal cord in rats with neuropathic pain [J]. Chin J Pain Med, 2015, 21(5): 335-340.

[19] KUNER R, FLOR H. Structural plasticity and reorganisation in chronic pain [J]. Nat Rev Neurosci, 2017, 18(2): 113.

[20] LIU Y, ZHOU L J, WANG J, et al. TNF-α differentially regulates synaptic plasticity in the hippocampus and spinal cord by microglia-dependent mechanisms after peripheral nerve injury [J]. J Neurosci, 2017, 37(4): 871-881.

[21] SUMIZONO M, YOSHIZATO Y, YAMAMOTO R, et al. Mechanisms of neuropathic pain and pain-relieving effects of exercise therapy in a rat neuropathic pain model [J]. J Pain Res, 2022, 15: 1925-1938.

[22] 李永男,车守梅,张祁,等. 米诺环素对神经病理性疼痛大鼠海马促炎性细胞因子表达的影响[J]. 医学研究杂志, 2019, 48(7): 54-58.
LI Y N, CHE S M, ZHANG Q, et al. Effect of minocycline on the expression of pro-inflammatory cytokines in hippocampus of rats with neuropathic pain [J]. J Med Res, 2019, 48(7): 54-58.

[23] 江孟鸿,张亮平,李长征,等. 电针环跳、阳陵泉对CCI大鼠海马^{18}F-FDG摄入率及GLUT-3表达的影响[J]. 福建中医药, 2021, 52(4): 20-22.
JIANG M H, ZHANG L P, LI C Z, et al. Effect of electroacupuncture at Huantiao (GB 30) and Yanglingquan (GB 34) on ^{18}F-FDG uptake and GLUT-3 expression in hippocampus of CCI rats [J]. Fujian J Tradit Chin Med, 2021, 52(4): 20-22.

[24] 张亮平,陈小梅,俞向梅,等. 电针环跳、阳陵泉穴对神经痛大鼠海马区NAA、Glu变化的影响[J]. 湖南中医杂志, 2020, 36(1): 126-128.
ZHANG L P, CHEN X M, YU X M, et al. Effect of electroacupuncture at Huantiao and Yanglingquan acupoints on the changes in N-acetylaspartate and glutamic acid in the hippocampus of rats with neuralgia [J]. Hunan J Tradit Chin Med, 2020, 36(1): 126-128.

[25] 王志福,俞向梅,姚冉冉,等. SD大鼠坐骨神经体表定位及相关针刺穴位的应用解剖研究[J]. 福建中医药大学学报, 2012, 22(6): 13-15.
WANG Z F, YU X M, YAO R R, et al. Applied anatomical study on surface location of SD rats sciatic nerve and related acupuncture points [J]. J Fujian Univ Tradit Chin Med, 2012, 22(6): 13-15.

[26] GONG D, YU X, JIANG M, et al. Differential proteomic analysis of the hippocampus in rats with neuropathic pain to investigate the use of electroacupuncture in relieving mechanical allodynia and cognitive decline [J]. Neural Plast, 2021, 2021: 5597163.

[27] WANG C, LIN G H, MCPHERSON A J, et al. Immune regulation by 4-1BB and 4-1BBL: complexities and challenges [J]. Immunol Rev, 2009, 229(1): 192-215.

[28] CROFT M. The role of TNF superfamily members in T-cell function and diseases [J]. Nat Rev Immunol, 2009, 9(4): 271-285.

[29] UGOLINI A, NUTI M. CD137^{+} T-cells: protagonists of the immunotherapy revolution [J]. Cancers (Basel), 2021, 13(3): 456.

[30] YEO Y A, MARTÍNEZ GÓMEZ J M, CROXFORD J L, et al. CD137 ligand activated microglia induces oligodendrocyte apoptosis via reactive oxygen species [J]. J Neuroinflammation, 2012, 9: 173.

[31] KANG Y J, KIM S O, SHIMADA S, et al. Cell surface 4-1BBL mediates sequential signaling pathways 'downstream' of TLR and is required for sustained TNF production in macrophages [J]. Nat Immunol, 2007, 8(6): 601-609.

Mechanism of Electroacupuncture on Neuropathic Pain via Regulation of CD137L in Hippocampal Glia

ZHENG Changyue[1], LAN Yanyan[2], HUANG Qiuling[2], JIANG Menghong[3], WANG Zhifu[2*]
[1] *Fujian Provincial Government Hospital, Fuzhou, Fujian 350003, China;*
[2] *Rehabilitation Hospital Affiliated to Fujian University of Traditional Chinese Medicine, Fuzhou, Fujian 350003, China;*
[3] *College of Acupuncture and Moxibustion, Fujian University of Traditional Chinese Medicine, Fuzhou, Fujian 350122, China*
*Correspondence: WANG Zhifu, E-mail: 2007015@fjtcm.edu.cn

ABSTRACT **Objective:** To investigate the mechanism of CD137L in CA1 region of hippocampus in improving mechanical pain and memory impairment in neuropathic pain rats during electroacupuncture therapy. **Methods:** A total of 24 SD rats were randomly divided into sham operation group, model group and electroacupuncture group, with 8 rats in each group. In the model and electroacupuncture groups, the spared nerve injury (SNI) model was made. The sham operation group was just exposed right sciatic nerve without ligation. From the 7th day after modeling, the electroacupuncture group received electroacupuncture intervention in the right side Huantiao (GB30) and Yanglingquan (G34) acupoints, 30 minutes each time, once a day, lasting for 21 days. Rats in the model and the sham operation groups were equally grasped and fixed without any intervention. Von-Frey pain detector was used to measure the mechanical withdrawal threshold of rats. On the 28th day after modeling, new object recognition test was used to detect the learning and memory ability. The expression of hippocampal CA1 region CD137L, Iba-1, GFAP and tumor necrosis factor-α (TNF-α) was detected by enzyme-linked immunosorbent assay (ELISA). Immunofluorescence was used for the cellular localization of CD137L and receptor CD137, and to measure the Iba-1 and GFAP expression in hippocampal CA1 region. **Results:** 1) Compared with the sham operation group, mechanical pain threshold and new object recognition index in the model group significantly decreased (P<0.01); compared with the model group, mechanical pain threshold and new object recognition index in the electroacupuncture group significantly increased (P<0.01). 2) Compared with the sham operation group, the concentrations of CD137L, Iba-1, GFAP and TNF-α in hippocampus of rats in the model group significantly increased (P<0.01), and the number of positive Iba-1 and GFAP immune reactions significantly increased (P<0.01); compared with the model group, the concentrations of CD137L, Iba-1, GFAP and TNF-α in hippocampus of rats in the electroacupuncture group significantly decreased (all P<0.05), and the number of positive immune reactions of Iba-1 and GFAP significantly decreased (all P<0.01). 3) Immunofluorescence detection showed that CD137L and its receptor CD137 were significantly co-expressed with microglia marker (Iba-1) and astrocyte marker (GFAP) in hippocampal CA1 region, suggesting that CD137L and CD137 were mainly expressed in microglia and astrocytes, but not in neurons. **Conclusion:** Electroacupuncture may play an analgesic role by reducing the expression of glial CD137L, the amount of activated glial cells and the concentrations of TNF-α.
KEY WORDS neuropathic pain; hippocampus; CD137L; glial cell; electroacupuncture
DOI:10.3724/SP.J.1329.2023.05005

（上接第 418 页）

Video Kinematic Analysis of Timed Up and Go Test in Convalescent Stroke Patients

CAI Tongxin[1,2], LEI Mincong[1], ZHOU Yijun[1], MENG Dianhuai[3*]
[1] *School of Rehabilitation Medicine, Nanjing Medical University, Nanjing, Jiangsu 210029, China;*
[2] *The First Affiliated Hospital of Xi'an Jiaotong University, Xi'an, Shaanxi 710061, China;*
[3] *The first Affiliated Hospital of Nanjing Medical University, Nanjing, Jiangsu 210029, China*
*Correspondence: MENG Dianhuai, E-mail: dhdream@126.com

ABSTRACT **Objective:** This study investigated and compared the results of the Timed Up and Go test (TUG test) between convalescent stroke patients and healthy controls by video recording, and the total time and sub-phase kinematic characteristics of the TUG test were analyzed to provide a theoretical basis for clinical application. Using the convenient sampling method, a total of 41 convalescent stroke patients were recruited as patient group (observation group) in the rehabilitation medical centers of three hospitals (including the First Affiliated Hospital of Nanjing Medical University, etc.) from June to September 2022. Additionally, 35 healthy people with gender, age, height and weight matched were selected as healthy control group (control group). The TUG test were recorded by cameras for all subjects. VirtualDube 2® software was used to analyze the kinematic characteristics of recorded video, including the total time and sub-stages parameters (stage 1 standing up, stage 2 forward walking, stage 3 first turning, stage 4 return walking, stage 5 end turning and sitting down); moreover, the observation group also received evaluation including five-times-sit-to-stand test, single leg support time and 10 m maximum walking speed. **Results:** Compared with the control group, the observation group had a significant increase in the time of total TUG [26.91(16.52, 35.98) s] and the sub-stages [1.98 (1.13, 2.48), 8.15 (4.21, 13.02), 4.15 (3.84, 5.93), 6.10 (3.08, 9.94), 5.04 (3.82, 7.03) s] (P<0.01), and there were significant differences in the percentage distribution of each sub-stage (P<0.05). There was a significant positive correlation between five-times-sit-to-stand test and time of total TUG test and each sub-stage in the observation group (P<0.01). There was a significant negative correlation between single leg support time of hemiplegic side and time of total TUG test and each sub-stage (P<0.01). There was a significant positive correlation between 10 m maximum walking speed and time of total TUG test and each sub-stage in the observation group (P<0.01). **Conclusion:** The TUG test video kinematics analysis can be used to accurately analyzing walking characteristics of patients in convalescent stroke patients, and corresponding sub-stage time can reflect the lower limb strength, standing balance, walking stability and other function of stroke patients.
KEY WORDS stroke; Timed Up and Go test; kinematics; video analysis; gait
DOI:10.3724/SP.J.1329.2023.05004